EVALUATING THE POTENTIALITIES OF COPERNICUS VERY HIGH RESOLUTION (VHR) OPTICAL DATASETS FOR ASSESSING THE SHORELINE EROSION HAZARD IN MICROTIDAL ENVIRONMENTS

L. Cenci [1 *], V. Pampanoni [2], G. Laneve [2], C. Santella [1], V. Boccia [3]

[1] Serco Italia SpA, Frascati, Italy - (luca.cenci, carla.santella)@serco.com
[2] Sapienza University of Rome, Rome, Italy - (valerio.pampanoni, giovanni.laneve)@uniroma1.it
[3] European Space Agency, Frascati, Italy - valentina.boccia@esa.int

KEY WORDS: Copernicus, Earth Observation (EO), Shoreline Erosion, Coastal Hazard and Risk, Very High Resolution (VHR)

ABSTRACT:

In the past years, several studies have shown that Earth Observation (EO) data can be successfully used for analysing shoreline evolution trends and assessing coastal erosion hazard/risk. Within this framework, the exploitation of long-term archives of sensors data characterised by moderate spatial resolution (e.g., Landsat) has shown its potential; particularly in higher energy coastal environments (e.g., Oceanic areas) where the magnitude of long-term erosion/accretion processes (e.g., decadal) can be resolved by the abovementioned sensors. However, the spatial resolution of these data may prevent an accurate analysis in microtidal coastal environments (e.g., Mediterranean Sea), especially for analyses focused on a short-term period (e.g., few years). This is mainly due to the high level of uncertainty associated with the occurrence of erosion/accretion processes of lower magnitude detected by EO sensors retaining a moderate spatial resolution. Within this context, this work was conceived to evaluate the potentialities of the Copernicus Very High Resolution (VHR) optical datasets (spatial resolution: 2-4 m) for assessing the shoreline evolution trends in an exemplifying urbanised coastal area of the Mediterranean Sea (i.e., Lido di Ostia, Rome, Italy), over a short-term period (i.e., 4 years). To achieve this objective, an automatic technique of shoreline detection and extraction at subpixel level was tested. Results allowed to: i) detect a shoreline evolution trend coherent with the geomorphological characteristics of the study area; ii) smoothly identify/quantify fine-scale variations of accretion/erosion patterns along the coast. This is extremely important to map the areas most exposed to shoreline erosion hazard/risk.

1. INTRODUCTION

In the past years, several studies proved the potentialities of using Earth Observation (EO) data for studying shoreline evolution through time (Apostolopoulos and Nikolakopoulos, 2021). These analyses are fundamental for Integrated Coastal Management (ICM) purposes and objectives: e.g., assessing the shoreline erosion hazard and risk; defining the most appropriate risk adaptation and mitigation strategies; monitoring the impact/effectiveness of coastal protection methods (e.g., hard structures, soft techniques, etc.). In this context, the exploitation of long-term archives of EO data acquired by sensors retaining a moderate spatial resolution (e.g., Landsat) has shown its potential; particularly in higher energy coastal environments (e.g., Oceanic areas) where the magnitude of long-term erosion/accretion processes (e.g., decadal) can be resolved by the abovementioned instruments. However, the spatial resolution of these data may prevent an accurate analysis in microtidal coastal environments (e.g., Mediterranean Sea), especially for short-term analyses (e.g., covering a time period of few years). This is mainly due to the high level of uncertainty associated with the occurrence of erosion/accretion processes of lower magnitude detected by EO sensors retaining a moderate spatial resolution (Cenci et al., 2018).

Considering the well-known issues related to the definition of the "true" shoreline concept, and the consequent practical complexities derived from its identification and mapping, the shoreline evolution through time is usually inferred by observing the advancement/retreat of specific coastal features called shoreline proxies: e.g., the Instantaneous Water Line (IWL), the base/top of bluff/cliff, the Stable Dune Vegetation Line (StDVL), etc. (Boak and Turner, 2005). One of the possible ways to map and monitor shoreline proxies through time is via EO data. In this case, standardised methodologies that guarantee their coherence in space and time should be used (Cenci et al., 2013). This is a fundamental prerequisite for performing reliable multitemporal analyses. The choice of the most suitable proxy to use for a given study area mostly depends on different factors: e.g., the geomorphological characteristics of the coast (e.g., if the dunes and/or the vegetation are present); the methodological approach used for their definition and mapping; the data availability (e.g., in case of EO images, the characteristics of the sensor used for acquiring the data).

Considering that the quantification of shoreline evolution trends (i.e., annual rate or total net movement of advance/retreat) is as reliable as the measurement (σ_m) and positional (σ_p) errors accounted for when mapping the exact position of the proxy, the quantification of the main uncertainty factors associated to the proxy extraction is of paramount importance (Fletcher et al., 2003; Himmelstoss et al., 2018). σ_m is related to operator-based factors, such as data source/s characteristics and data processing (e.g., spatial resolution of the sensor and orthorectification accuracy, in case of EO-based analyses). σ_p is related to the factors influencing the definition of the real proxy position during a given year (e.g., tide and waves influence on the shoreline position etc.). These uncertainties are assumed to be random, not correlated and can be used to quantify an overall total uncertainty (σ_{tot}) (Fletcher et al., 2003).

Within this framework, this work was conceived to evaluate the potentialities of the Copernicus Very High Resolution (VHR) datasets (ESA, 2021) for assessing the shoreline evolution trends in an exemplifying coastal area of the Mediterranean Sea over a short-term period (i.e., 4 years). Considering that the EO

* Corresponding author

data used for the analysis have a spatial resolution (i.e., Ground Sampling Distance - GSD) of ca. 2 m, this work aims at evaluating their potential for performing such analysis in a microtidal environment where the occurrence of erosion/accretion processes of (relatively) low(er) magnitude (e.g., if compared against the ones occurring in Oceanic areas) may be accurately detected by taking advantage of VHR data. Indeed, the images used for the aforementioned analysis are characterised by a (relatively) low(er) σ_m, because this parameter is strongly influenced by the spatial resolution of the instrument used for acquiring the data. This is particularly important for performing the shoreline erosion hazard assessment in coastal zones characterised by a strong anthropic influence, as is usually the case in the Mediterranean area. Indeed, in such places, erosive processes may produce strong economic damages to the exposed assets (e.g., business activities, public and private properties, etc.). To this aim, the analysis presented in this paper was carried out in Lido di Ostia, which is the coastal district of the city of Rome (Italy). As such, the area is characterised by assets potentially exposed to the shoreline erosion hazard and risk. Analysis results were thus interpreted by taking into account the geomorphological characteristics of the coast and in an Integrated Coastal Management (ICM) framework.

2. STUDY AREA AND DATA SOURCE

The study area selected for performing the analysis described in this paper is the coastal area of the city of Rome (Italy): Lido di Ostia (Figure 1). This district is located on the Tyrrhenian Sea and it is ca. 25 km far from the Rome city centre. A detailed description of the study area can be found in Ferrante et al. (1992) and Tomasicchio (1996). Instead, the information most relevant for the presented analyses is summarised below. Lido di Ostia is characterised by a typical Mediterranean climate. The local tidal range is small (i.e., < 0.5 m), but deep-water waves may exceed a significant height of 5 m and a period of 10 s. The longshore current is directed southwards. The littoral (length: ca. 20 km) is composed by sandy beaches, that stretch along the southern delta cusp of the Tiber River. The shoreline continuity is interrupted by a touristic harbour (located in the northernmost part of the study area), and by an artificial channel (width: ca. 20 m) named Canale dei Pescatori (located in the central part of the study area). The geomorphological evolution of the coastal environment has been strongly influenced by the Tiber. From the ‘50s onwards, erosive processes affected the study area. These were mainly originated by the strong reduction of the sediment load transported by the river (due to upstream dams and extraction of building material from the riverbed), with a subsequent deficit in the coastal sand budget. Being Lido di Ostia the *de facto* coastal district of the Italian capital city (i.e., Rome), it is characterised by strong anthropic pressure. This translates into a high concentration of vulnerable assets and economic activities exposed to coastal risk induced by the shoreline erosion hazard. This is particularly true in the northern and in the central parts of the study area, where the coast is strongly urbanised and the dunal/vegetation system has been destroyed and replaced by anthropic buildings and features; thus, removing the natural protection of the beach from coastal risk. Instead, in the southern part of the study area, the natural environment of the coast (including the dunal/vegetation system) have been preserved. In this part, the presence of anthropic assets and economic activities can be considered negligible with respect to the northern and central part. Since the ‘70s, different defence structures and protective strategies were set up in the northern and central parts to reduce the impact of the shoreline erosion hazard on the exposed assets. Hard defence structures were mostly built in the northern part. Instead, soft defence structures and nourishment strategies were typically preferred in the central one. Within this context, it is important to highlight that the inlet of the Canale dei Pescatori acts as a groyne that affects the sediment transport capacity of the longshore current. This generated strong erosion problems in the coastal areas located to the South of the Canale dei Pescatori, that in turn caused economic damages to the beach clubs and even to the littoral road during storm periods.

The satellite data used for performing the analysis described in this paper are part of the Copernicus VHR 2015 and 2018 datasets. The Copernicus VHR datasets provide, every 3±1 years, a cloud-free coverage of Europe (EEA39 area) derived from optical sensors retaining a GSD ranging between 2 and 4 m. The data are acquired by selected Copernicus Contributing Missions (CCMs) during the vegetation season of the reference year of the dataset (e.g., 2015, 2018, etc.), ±1 year for ensuring the full coverage of the target area. All the CCMs have similar characteristics (e.g., in terms of geometric, radiometric and spectral resolutions) and provide multispectral data in the visible (blue, green and red spectral bands) and Near InfraRed (NIR) interval of the electromagnetic spectrum. These data are then processed to generate products geometrically and radiometrically consistent across the same (and other) VHR dataset(s). The latter are then distributed with two different: i) pixel sizes (i.e., 2 and 4 m, according to the different, native GSDs of the sensors used for acquiring the data); ii) processing levels (i.e., ortho-ready and orthorectified). The VHR dataset products are accompanied by comprehensive metadata that provide relevant information to the users, for instance: i) the parameters needed to calibrate the data to Top Of Atmosphere (TOA) radiance and reflectance (ρ); ii) the accuracy of the orthorectification process (expressed in terms of Root Mean Square Error - RMSE), for orthorectified products; etc. Further information about Copernicus VHR datasets can be found in ESA (2021). Concerning the work described in this paper, the images used for performing the analysis were acquired in July 2014 (VHR 2015 dataset) and June, July and August 2018 (VHR 2018 dataset). In the first case, only 1 image was sufficient for covering the whole study area. In the second case, 3 images were required. All the products used for the analysis were distributed with a pixel size of 2 m.

3. METHODOLOGY

Concerning the choice of the coastal feature to use as shoreline proxy, the one selected for the analysis was the IWL: i.e., the position of the beach–sea boundary at an instant in time (Boak and Turner, 2005). With respect to vegetation-based proxy (e.g., StDVL) this feature is characterised by a higher level of uncertainty because its σ_p is influenced by different factors, such as tide and waves effects (Cenci et al., 2018). However, considering the characteristics of the study area (i.e., absence of dunal/vegetation system in the northern and central parts), it was the only viable option.

The following analyses were performed on subset areas of the VHR dataset products. These subsets were obtained by: i) downloading the European Environment Agency (EEA) coastline dataset (from https://www.eea.europa.eu/) as a vector (polyline) layer; ii) clipping it on the extent of the study area; iii) creating a 1 km buffer layer (i.e., 500 m seaward and 500 m landward); iv) using the buffer layer to cut the subsets from all the images. Then, the subset images were calibrated to TOA ρ by using the required information provided in the product metadata. Subsequently, the Normalised Difference Water

Index (NDWI) was computed for every image by using the green and the NIR spectral bands (Bishop-Taylor et al., 2019). Since NDWI values range from -1.0 (land) to 1.0 (water), a threshold value must be defined to identify the beach–sea boundary. To account for possible differences in the radiometric response (i.e., TOA ρ values) of the coastal environment in different acquisition days (e.g., due to diverse atmospheric and weather-related conditions), the Otsu method was used for performing an automatic threshold selection for each product under analysis (Bishop-Taylor et al., 2019). Indeed, this method allowed to coherently extract the same feature (i.e., the IWL), in different images, by using different threshold values identified by exploiting a statistical approach. Consequently, a specific threshold value was computed for every single NDWI image by considering the statistical distribution of its land/water pixels present in the coastal area. To take into account the Otsu assumption of bimodality, the portion of the coastal areas to use for the threshold selection was defined by creating a buffer of 60 m (i.e., 30 m seaward and 30 m landward) from each side of the "first guess" coastline. The "first guess" coastline was extracted by segmenting the NDWI subset image via the K-means algorithm (with K=2). Then, the IWL was automatically extracted with subpixel precision as a vector (polyline) layer, from every NDWI image, by using the marching squares approach with linear interpolation algorithm (Bishop-Taylor et al., 2019). This method linearly interpolates between the NDWI values of neighbouring pixels to identify the exact location of the IWL according to a specified threshold value (i.e., the one that was previously estimated, for every image, via Otsu). Afterwards, the IWL vector layers were edited to remove local inaccuracies due to the extraction processes. Finally, the 3 IWL layers extracted from the VHR 2018 dataset images were merged to create a single IWL referred to 2018. Since the whole 2014 IWL was extracted from a single product, this step was not required for the 2014 case. The overall total uncertainty (σ_{tot}) associated with the 2014 and 2018 IWLs was estimated by following the approach used by Virdis et al. (2012) and Cenci et al. (2018). Consequently, the factors determining σ_m were: i) the spatial resolution error (σ_{sr}); ii) the orthorectification error (σ_o). The factors determining σ_p were: iii) the tidal fluctuation error (σ_t); iv) the wave fluctuation error (σ_w). σ_t and σ_w were taken into account for considering possible fluctuations in IWL positions depending on variations in tide and wave height levels. Although the IWLs were extracted by using a subpixel approach, σ_{sr} was approximated to the pixel size of the images (i.e., 2 m). σ_o was calculated as the mean of the RMSE values reported in the metadata of the products (i.e., 1.96 m). σ_t was estimated as the projection of the standard deviation of the mean tidal level (i.e., 0.09 m) on the beach slope. Tidal measurements were recorded by the Civitavecchia Harbour tide gauge station (located ca. 60 km North of the study area) in the 2011–2020 summertime (i.e., from June to August). Data were downloaded from https://www.mareografico.it/. σ_w was estimated as the projection of the standard deviation of the mean wave height (i.e., 0.38 m) on the beach slope. Wave height measurements were recorded by the Civitavecchia buoy in the 2002–2014 summertime. Data were downloaded from http://dati.isprambiente.it/. For both σ_t and σ_w, the beach slope was obtained by using the Copernicus Digital Elevation Model (COP-DEM) dataset (ESA, 2021; Cenci et al., 2021). More precisely, the EEA-10 (DGED) instance of the COP-DEM dataset was used (spatial resolution: ca. 12 m). The beach slope of the study area (ca. 3°) was estimated as the average slope value computed over the last 15 m before the COP-DEM shoreline (i.e., the boundary between land and sea represented on the COP-DEM). The values attributed to σ_t and σ_w correspond to 1.8 m and 7.26 m, respectively. Following Fletcher et al. (2003), the overall total uncertainty was calculated as the square root of the sum of the squares of all the above-mentioned uncertainty factors (i.e., σ_{sr}, σ_o, σ_t, σ_w). Therefore, $\pm\sigma_{tot}$ value is ±8 m.

The 2014 and 2018 IWLs vector layers were then used to analyse the shoreline net movements and evolution trends along equally spaced transects cast every 2 m perpendicularly to the shore. The elaboration was performed by means of the Digital Shoreline Analysis System (DSAS), a freely available application that works within the ESRI ArcGIS software (Himmelstoss et al., 2018). DSAS allowed us to compute the Net Shoreline Movement (NSM): i.e., the distance between the oldest (2014) and the youngest (2018) IWL for each transect (unit: m). If this distance is divided by the time elapsed between the two proxy positions (i.e., 4 years), the result is the End Point Rate (EPR): i.e., the rate of change associated with the shoreline movements (unit: m/y). In both cases, positive values are associated with transects where the shoreline advanced; negative values are associated with transects where the shoreline retreated. The latter can be linked with areas characterised by erosive processes.

4. RESULTS

The results of the analysis are shown in Figure 1, where the NSM and EPR values of each transect are displayed. A red-to-green colour scale was used to highlight trends of retreat or advancement, respectively. Additionally, a binary colour scale classification was used to identify 2 typologies of transects: "Type 1" are transects whose NSM ranges between $\pm\sigma_{tot}$ (displayed in black); "Type 2" are transects whose NSM is $< -\sigma_{tot}$ or $> +\sigma_{tot}$ (displayed in white).

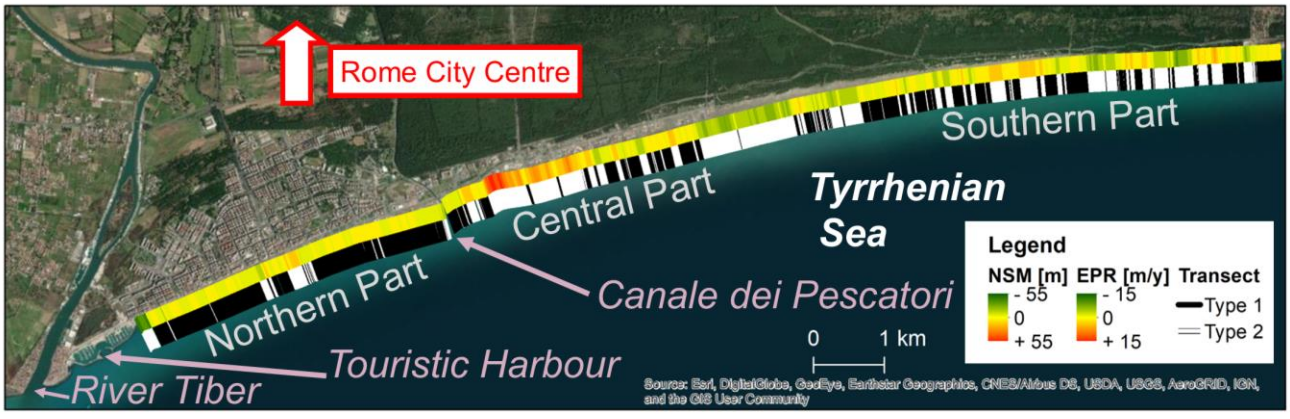

Figure 1 The figure shows the study area and the results of the analysis (i.e., NSM and EPR values associated to each transect).

5. DISCUSSION AND CONCLUSIONS

By observing Figure 1 it can be stated that, in the time period under investigation, the northern part of the study area was characterised by an advancement of the shoreline. This can be mostly explained by the stronger presence of hard defence structures. Nevertheless, the analysis still highlighted some small areas (i.e., cluster of neighbouring transects) characterised by erosive processes, and thus exposed to coastal erosion risk. The strongest shoreline advance was observed in the northernmost part of the study areas, nearby the touristic harbour. The greatest erosive processes, instead, were recorded in the central part of the study area, more precisely South of the Canale dei Pescatori. In the past decades this zone has been known to be affected by shoreline erosion hazard (Ferrante et al., 1992; Tomasicchio, 1996) and, considering the presence of the vulnerable assets, it can be still considered highly exposed to coastal risk. In the remaining part of the central area and in the southern one, an alternation of zones characterised by erosive and accretion processes can be observed, with a prevalence of the latter. Because of the lack of recent studies carried out to evaluate the shoreline evolution dynamics of the study area with analogous methodologies, a quantitative validation of the results was not possible. However, the analysis of NSM and EPR values derived from VHR data allowed us to detect a shoreline evolution trend coherent with the geomorphological characteristics of the study area and previous literature findings (Ferrante et al., 1992; Tomasicchio, 1996). Importantly, the joint exploitation of VHR data and the automatic subpixel approach used for extracting the shoreline proxy allowed us to smoothly identify fine-scale variations of accretion/erosion patterns along the coast. This is extremely important for ICM purposes and objectives. The presented analysis also showed a not negligible percentage of "Type 1" transects: ca. 55%. These transects can be associated with areas in which the differences between the 2014 and 2018 IWL positions can be largely influenced by σ_{tot} factors, rather than associated with proper shoreline evolution dynamics. However, the exploitation of Copernicus VHR datasets allowed us to lower the percentage of "Type 1" transects, by reducing σ_m contribution in σ_{tot}. Since the characteristic of the study area imposed the choice of the IWL as proxy, the (relatively) large(r) contribution of σ_p in σ_{tot} prevented a further reduction of the overall total uncertainty of the analysis, and thus of the percentage of "Type 1" transects.

To conclude, the results of the analysis presented in this paper showed the potential of the Copernicus VHR datasets for shoreline evolution analyses in microtidal environments carried out over a short period of time. Findings also highlighted one of the societal benefits that can be achieved via the Copernicus programme (e.g., to support ICM). Future studies are encouraged to further evaluate the potentialities of the Copernicus VHR datasets for performing analyses similar to the one presented in this paper, but carried out in coastal areas characterised by different environmental characteristics (e.g., mesotidal and macrotidal environments) to: i) confirm the findings of the presented research; ii) evaluate the VHR data potential for multi-proxy analyses, if possible (Cenci et al., 2018). Moreover, follow up activities are also suggested to test the performance of the automatic subpixel approach used for extracting the proxy when applied to EO data characterised by lower spatial resolution but higher temporal resolution (e.g., Sentinel 2 and Landsat data) in similar case studies. Importantly, for these future analyses, shoreline evolution trends obtained by exploiting Copernicus VHR datasets can be used as reference data to validate the results.

ACKNOWLEDGEMENTS

Activity carried out by the Copernicus Coordinated data Quality Control (CQC) service - run by Serco Italia SpA - and La Sapienza University of Rome within the ESA PRISM contract.

REFERENCES

Apostolopoulos, D., and Nikolakopoulos, K., 2021. A Review and Meta-Analysis of Remote Sensing Data, GIS Methods, Materials and Indices Used for Monitoring the Coastline Evolution over the Last Twenty Years. *European Journal of Remote Sensing*, 54(1), pp. 240–265. doi:10.1080/22797254.2021.1904293

Bishop-Taylor, R., et al., 2019. Sub-Pixel Waterline Extraction: Characterising Accuracy and Sensitivity to Indices and Spectra. *Remote Sensing*, 11(24), 2984. doi:10.3390/rs11242984

Boak, E.H., and Turner, I.L., 2005. Shoreline Definition and Detection: A Review. *Journal of Coastal Research*, 21(4), pp. 688–703. doi:10.2112/03-0071.1

Cenci, L., et al., 2018. Integrating Remote Sensing and GIS Techniques for Monitoring and Modeling Shoreline Evolution to Support Coastal Risk Management. *GIScience and Remote Sensing*, 55(3), pp. 355–375. https://doi.org/10.1080/15481603.2017.1376370

Cenci, L., et al., 2013. Geomatics for Integrated Coastal Zone Management: Multitemporal Shoreline Analysis and Future Regional Perspective for the Portuguese Central Region. *Journal of Coastal Research*, 65, pp. 1349–1354. https://doi.org/10.2112/SI65-228.1

Cenci, L., et al., 2021. Describing the Quality Assessment Workflow Designed for DEM Products Distributed via the Copernicus Programme. Case Study: The Absolute Vertical Accuracy of the Copernicus DEM Dataset in Spain. *In: Proceedings of the 2021 IEEE International Geoscience and Remote Sensing Symposium (IGARSS), Brussels, Belgium, 2021*, pp. 6143-6146.

ESA, 2021. Copernicus Space Component Data Access Portfolio: Data Warehouse 2014 - 2022. https://copernicusdata.esa.int/web/cscda/home

Ferrante, A., et al., 1992. Modelling and Monitoring of a Perched Beach at Lido Di Ostia (Rome). *Coastal Engineering 1992*, pp., 3305–3318. doi:10.1061/9780872629332.251

Fletcher, C., et al., 2003. Mapping Shoreline Change Using Digital Orthophotogrammetry on Maui, Hawaii. *Journal of Coastal Research*, 38, pp. 106–124. https://www.jstor.org/stable/25736602

Himmelstoss, E.A., et al., 2018. Digital Shoreline Analysis System (DSAS) Version 5.0. *U.S. Geological Survey Open-File Report 2018–1179*, doi:https://doi.org/10.3133/ ofr20181179

Tomasicchio, U., 1996. Submerged Breakwaters for the Defence of the Shoreline at Ostia Field Experiences, Comparison. *Coastal Engineering 1996*, pp. 2404-2417. doi:10.1061/9780784402429.186

Virdis, S.G.P., et al., 2012. A Geomatics Approach to Multitemporal Shoreline Analysis in Western Mediterranean: The Case of Platamona-Maritza Beach (Northwest Sardinia, Italy). *Journal of Coastal Research*, 28(3), pp. 624–640. doi:10.2112/JCOASTRES-D-11-00078.1